

Measurement of the B^+ and B^0 Lifetimes from Semileptonic Decays*

The SLD Collaboration
Stanford Linear Accelerator Center,
Stanford University, Stanford, CA 94309

Abstract

The lifetimes of B^+ and B^0 mesons are measured using a sample of 150,000 hadronic Z^0 decays collected by the SLD experiment at the SLC between 1993 and 1995. The analysis identifies the semileptonic decays of B mesons and reconstructs the B meson decay length and charge by vertexing the lepton with a partially reconstructed D meson. This new method results in a sample of 634 (584) charged (neutral) decays with high charge purity. The ratio of $B^+ : B^0$ decays in the charged (neutral) sample is 3:1 (1:3). A maximum likelihood fit yields $\tau_{B^+} = 1.61^{+0.13}_{-0.12}(\text{stat}) \pm 0.07(\text{syst})$ ps, $\tau_{B^0} = 1.56^{+0.14}_{-0.13} \pm 0.10$ ps, and $\tau_{B^+}/\tau_{B^0} = 1.03^{+0.16}_{-0.14} \pm 0.09$.

Submitted to *Physical Review Letters*

*Work supported in part by the Department of Energy contract DE-AC03-76SF00515.

K. Abe,⁽¹⁹⁾ K. Abe,⁽³⁰⁾ T. Akagi,⁽²⁸⁾ N.J. Allen,⁽⁴⁾ W.W. Ash,^{(28)†}
 D. Aston,⁽²⁸⁾ K.G. Baird,⁽¹⁶⁾ C. Baltay,⁽³⁴⁾ H.R. Band,⁽³³⁾ M.B. Barakat,⁽³⁴⁾
 G. Baranko,⁽⁹⁾ O. Bardon,⁽¹⁵⁾ T. L. Barklow,⁽²⁸⁾ G.L. Bashindzhagyan,⁽¹⁸⁾
 A.O. Bazarko,⁽¹⁰⁾ R. Ben-David,⁽³⁴⁾ A.C. Benvenuti,⁽²⁾ G.M. Bilei,⁽²²⁾
 D. Bisello,⁽²¹⁾ G. Blaylock,⁽¹⁶⁾ J.R. Bogart,⁽²⁸⁾ B. Bolen,⁽¹⁷⁾ T. Bolton,⁽¹⁰⁾
 G.R. Bower,⁽²⁸⁾ J.E. Brau,⁽²⁰⁾ M. Breidenbach,⁽²⁸⁾ W.M. Bugg,⁽²⁹⁾
 D. Burke,⁽²⁸⁾ T.H. Burnett,⁽³²⁾ P.N. Burrows,⁽¹⁵⁾ W. Busza,⁽¹⁵⁾
 A. Calcaterra,⁽¹²⁾ D.O. Caldwell,⁽⁵⁾ D. Calloway,⁽²⁸⁾ B. Camanzi,⁽¹¹⁾
 M. Carpinelli,⁽²³⁾ R. Cassell,⁽²⁸⁾ R. Castaldi,^{(23)(a)} A. Castro,⁽²¹⁾
 M. Cavalli-Sforza,⁽⁶⁾ A. Chou,⁽²⁸⁾ E. Church,⁽³²⁾ H.O. Cohn,⁽²⁹⁾
 J.A. Coller,⁽³⁾ V. Cook,⁽³²⁾ R. Cotton,⁽⁴⁾ R.F. Cowan,⁽¹⁵⁾ D.G. Coyne,⁽⁶⁾
 G. Crawford,⁽²⁸⁾ A. D'Oliveira,⁽⁷⁾ C.J.S. Damerell,⁽²⁵⁾ M. Daoudi,⁽²⁸⁾
 R. De Sangro,⁽¹²⁾ R. Dell'Orso,⁽²³⁾ P.J. Dervan,⁽⁴⁾ M. Dima,⁽⁸⁾
 D.N. Dong,⁽¹⁵⁾ P.Y.C. Du,⁽²⁹⁾ R. Dubois,⁽²⁸⁾ B.I. Eisenstein,⁽¹³⁾ R. Elia,⁽²⁸⁾
 E. Etzion,⁽³³⁾ S. Fahey,⁽⁹⁾ D. Falciari,⁽²²⁾ C. Fan,⁽⁹⁾ J.P. Fernandez,⁽⁶⁾
 M.J. Fero,⁽¹⁵⁾ R. Frey,⁽²⁰⁾ K. Furuno,⁽²⁰⁾ T. Gillman,⁽²⁵⁾ G. Gladding,⁽¹³⁾
 S. Gonzalez,⁽¹⁵⁾ E.L. Hart,⁽²⁹⁾ J.L. Harton,⁽⁸⁾ A. Hasan,⁽⁴⁾ Y. Hasegawa,⁽³⁰⁾
 K. Hasuko,⁽³⁰⁾ S. J. Hedges,⁽³⁾ S.S. Hertzbach,⁽¹⁶⁾ M.D. Hildreth,⁽²⁸⁾
 J. Huber,⁽²⁰⁾ M.E. Huffer,⁽²⁸⁾ E.W. Hughes,⁽²⁸⁾ H. Hwang,⁽²⁰⁾ Y. Iwasaki,⁽³⁰⁾
 D.J. Jackson,⁽²⁵⁾ P. Jacques,⁽²⁴⁾ J. A. Jaros,⁽²⁸⁾ A.S. Johnson,⁽³⁾
 J.R. Johnson,⁽³³⁾ R.A. Johnson,⁽⁷⁾ T. Junk,⁽²⁸⁾ R. Kajikawa,⁽¹⁹⁾
 M. Kalelkar,⁽²⁴⁾ H. J. Kang,⁽²⁶⁾ I. Karliner,⁽¹³⁾ H. Kawahara,⁽²⁸⁾
 H.W. Kendall,⁽¹⁵⁾ Y. D. Kim,⁽²⁶⁾ M.E. King,⁽²⁸⁾ R. King,⁽²⁸⁾ R.R. Koffler,⁽¹⁶⁾
 N.M. Krishna,⁽⁹⁾ R.S. Kroeger,⁽¹⁷⁾ J.F. Labs,⁽²⁸⁾ M. Langston,⁽²⁰⁾
 A. Lath,⁽¹⁵⁾ J.A. Lauber,⁽⁹⁾ D.W.G.S. Leith,⁽²⁸⁾ V. Lia,⁽¹⁵⁾ M.X. Liu,⁽³⁴⁾
 X. Liu,⁽⁶⁾ M. Loreti,⁽²¹⁾ A. Lu,⁽⁵⁾ H.L. Lynch,⁽²⁸⁾ J. Ma,⁽³²⁾
 G. Mancinelli,⁽²²⁾ S. Manly,⁽³⁴⁾ G. Mantovani,⁽²²⁾ T.W. Markiewicz,⁽²⁸⁾
 T. Maruyama,⁽²⁸⁾ H. Masuda,⁽²⁸⁾ E. Mazzucato,⁽¹¹⁾ A.K. McKemey,⁽⁴⁾
 B.T. Meadows,⁽⁷⁾ R. Messner,⁽²⁸⁾ P.M. Mockett,⁽³²⁾ K.C. Moffeit,⁽²⁸⁾
 T.B. Moore,⁽³⁴⁾ D. Muller,⁽²⁸⁾ T. Nagamine,⁽²⁸⁾ S. Narita,⁽³⁰⁾
 U. Nauenberg,⁽⁹⁾ H. Neal,⁽²⁸⁾ M. Nussbaum,⁽⁷⁾ Y. Ohnishi,⁽¹⁹⁾
 L.S. Osborne,⁽¹⁵⁾ R.S. Panvini,⁽³¹⁾ C.H. Park,⁽²⁷⁾ H. Park,⁽²⁰⁾ T.J. Pavel,⁽²⁸⁾
 I. Peruzzi,^{(12)(b)} M. Piccolo,⁽¹²⁾ L. Piemontese,⁽¹¹⁾ E. Pieroni,⁽²³⁾
 K.T. Pitts,⁽²⁰⁾ R.J. Plano,⁽²⁴⁾ R. Prepost,⁽³³⁾ C.Y. Prescott,⁽²⁸⁾
 G.D. Punkar,⁽²⁸⁾ J. Quigley,⁽¹⁵⁾ B.N. Ratcliff,⁽²⁸⁾ T.W. Reeves,⁽³¹⁾
 J. Reidy,⁽¹⁷⁾ P.L. Reinertsen,⁽⁶⁾ P.E. Rensing,⁽²⁸⁾ L.S. Rochester,⁽²⁸⁾

P.C. Rowson,⁽¹⁰⁾ J.J. Russell,⁽²⁸⁾ O.H. Saxton,⁽²⁸⁾ T. Schalk,⁽⁶⁾
 R.H. Schindler,⁽²⁸⁾ B.A. Schumm,⁽⁶⁾ S. Sen,⁽³⁴⁾ V.V. Serbo,⁽³³⁾
 M.H. Shaevitz,⁽¹⁰⁾ J.T. Shank,⁽³⁾ G. Shapiro,⁽¹⁴⁾ D.J. Sherden,⁽²⁸⁾
 K.D. Shmakov,⁽²⁹⁾ C. Simopoulos,⁽²⁸⁾ N.B. Sinev,⁽²⁰⁾ S.R. Smith,⁽²⁸⁾
 M.B. Smy,⁽⁸⁾ J.A. Snyder,⁽³⁴⁾ P. Stamer,⁽²⁴⁾ H. Steiner,⁽¹⁴⁾ R. Steiner,⁽¹⁾
 M.G. Strauss,⁽¹⁶⁾ D. Su,⁽²⁸⁾ F. Suekane,⁽³⁰⁾ A. Sugiyama,⁽¹⁹⁾ S. Suzuki,⁽¹⁹⁾
 M. Swartz,⁽²⁸⁾ A. Szumilo,⁽³²⁾ T. Takahashi,⁽²⁸⁾ F.E. Taylor,⁽¹⁵⁾
 E. Torrence,⁽¹⁵⁾ A.I. Trandafir,⁽¹⁶⁾ J.D. Turk,⁽³⁴⁾ T. Usher,⁽²⁸⁾ J. Va'vra,⁽²⁸⁾
 C. Vannini,⁽²³⁾ E. Vella,⁽²⁸⁾ J.P. Venuti,⁽³¹⁾ R. Verdier,⁽¹⁵⁾ P.G. Verdini,⁽²³⁾
 D.L. Wagner,⁽⁹⁾ S.R. Wagner,⁽²⁸⁾ A.P. Waite,⁽²⁸⁾ S.J. Watts,⁽⁴⁾
 A.W. Weidemann,⁽²⁹⁾ E.R. Weiss,⁽³²⁾ J.S. Whitaker,⁽³⁾ S.L. White,⁽²⁹⁾
 F.J. Wickens,⁽²⁵⁾ D.A. Williams,⁽⁶⁾ D.C. Williams,⁽¹⁵⁾ S.H. Williams,⁽²⁸⁾
 S. Willocq,⁽²⁸⁾ R.J. Wilson,⁽⁸⁾ W.J. Wisniewski,⁽²⁸⁾ M. Woods,⁽²⁸⁾
 G.B. Word,⁽²⁴⁾ J. Wyss,⁽²¹⁾ R.K. Yamamoto,⁽¹⁵⁾ J.M. Yamartino,⁽¹⁵⁾
 X. Yang,⁽²⁰⁾ J. Yashima,⁽³⁰⁾ S.J. Yellin,⁽⁵⁾ C.C. Young,⁽²⁸⁾ H. Yuta,⁽³⁰⁾
 G. Zapalac,⁽³³⁾ R.W. Zdarko,⁽²⁸⁾ and J. Zhou,⁽²⁰⁾

(The SLD Collaboration)

- ⁽¹⁾ *Adelphi University, Garden City, New York 11530*
⁽²⁾ *INFN Sezione di Bologna, I-40126 Bologna, Italy*
⁽³⁾ *Boston University, Boston, Massachusetts 02215*
⁽⁴⁾ *Brunel University, Uxbridge, Middlesex UB8 3PH, United Kingdom*
⁽⁵⁾ *University of California at Santa Barbara, Santa Barbara, California*
 93106
⁽⁶⁾ *University of California at Santa Cruz, Santa Cruz, California 95064*
⁽⁷⁾ *University of Cincinnati, Cincinnati, Ohio 45221*
⁽⁸⁾ *Colorado State University, Fort Collins, Colorado 80523*
⁽⁹⁾ *University of Colorado, Boulder, Colorado 80309*
⁽¹⁰⁾ *Columbia University, New York, New York 10027*
⁽¹¹⁾ *INFN Sezione di Ferrara and Università di Ferrara, I-44100 Ferrara,*
 Italy
⁽¹²⁾ *INFN Lab. Nazionali di Frascati, I-00044 Frascati, Italy*
⁽¹³⁾ *University of Illinois, Urbana, Illinois 61801*
⁽¹⁴⁾ *Lawrence Berkeley Laboratory, University of California, Berkeley,*
 California 94720

- (15) *Massachusetts Institute of Technology, Cambridge, Massachusetts 02139*
 (16) *University of Massachusetts, Amherst, Massachusetts 01003*
 (17) *University of Mississippi, University, Mississippi 38677*
 (18) *Moscow State University, Institute of Nuclear Physics 119899 Moscow, Russia*
 (19) *Nagoya University, Chikusa-ku, Nagoya 464 Japan*
 (20) *University of Oregon, Eugene, Oregon 97403*
 (21) *INFN Sezione di Padova and Università di Padova, I-35100 Padova, Italy*
 (22) *INFN Sezione di Perugia and Università di Perugia, I-06100 Perugia, Italy*
 (23) *INFN Sezione di Pisa and Università di Pisa, I-56100 Pisa, Italy*
 (24) *Rutgers University, Piscataway, New Jersey 08855*
 (25) *Rutherford Appleton Laboratory, Chilton, Didcot, Oxon OX11 0QX United Kingdom*
 (26) *Sogang University, Seoul, Korea*
 (27) *Soongsil University, Seoul, Korea 156-743*
 (28) *Stanford Linear Accelerator Center, Stanford University, Stanford, California 94309*
 (29) *University of Tennessee, Knoxville, Tennessee 37996*
 (30) *Tohoku University, Sendai 980 Japan*
 (31) *Vanderbilt University, Nashville, Tennessee 37235*
 (32) *University of Washington, Seattle, Washington 98195*
 (33) *University of Wisconsin, Madison, Wisconsin 53706*
 (34) *Yale University, New Haven, Connecticut 06511*

† *Deceased*

(a) *Also at the Università di Genova*

(b) *Also at the Università di Perugia*

According to the spectator model of heavy hadron weak decay, the heavy quark decays independently of the other quarks in the hadron. Therefore, this model predicts that the lifetimes of all hadrons containing a given heavy quark Q are equal. However, the hierarchy observed in the charm system, $\tau_{D^+} > \tau_{D_s^+} \sim \tau_{D^0} > \tau_{\Lambda_c^+}$, indicates the need for corrections to this model. Such lifetime differences are predicted to scale with $1/m_Q^2$ [1] and therefore are expected to be less than 10% in the b -quark system. Measurements of the B^+ and B^0 lifetimes provide tests of this prediction. Finally, precise measurements of exclusive B meson lifetimes are necessary to extract the CKM matrix element V_{cb} .

The measurements presented here use a sample of 150,000 hadronic Z^0 decays collected between 1993 and 1995 by the SLD experiment at the SLC. The analysis uses a new technique to identify the B hadron charge by reconstructing the charged track topology of both B and cascade D vertices in semileptonic B decays. Most previous measurements of the B^+ and B^0 lifetimes [2] are based on samples of semileptonic decays in which the lepton is identified and the $D^{(*)}$ meson is fully reconstructed. The lifetime measurements then rely on assumptions concerning the B^+ and B^0 content of the $\overline{D^0} X l^+ \nu$ and $D^{(*)-} X l^+ \nu$ samples. In contrast, the more inclusive technique used here only relies on the simple difference of total charge between B^+ and B^0 decays. However, this technique requires very good vertexing to assign tracks correctly to secondary vertices.

The analysis uses the calorimetry and tracking systems (for details see Ref. [3]). The Liquid Argon Calorimeter (LAC) is used to reconstruct jets from energy clusters and perform electron identification with maximal efficiency for $|\cos \theta| < 0.72$. The Warm Iron Calorimeter (WIC) provides efficient muon identification for $|\cos \theta| < 0.60$. Tracking is performed with the Central Drift Chamber (CDC) and the CCD pixel Vertex Detector (VXD) with 94% total reconstruction efficiency for $|\cos \theta| < 0.74$ (including VXD hit linking). The impact parameter resolution for high-momentum tracks is measured using $Z^0 \rightarrow \mu^+ \mu^-$ decays to be 11 μm in the plane perpendicular to the beam axis ($r\phi$ plane) and 38 μm in the plane containing the beam axis (rz plane).

The decay length is measured relative to the position of the micron-size SLC Interaction Point (IP) which is reconstructed in the $r\phi$ plane with a precision of $\sigma_{r\phi} = (7 \pm 2) \mu\text{m}$ using tracks in sets of ~ 30 sequential hadronic Z^0 decays. The z position of the IP is determined on an event-by-event basis

with $\sigma_z \simeq 52 \mu\text{m}$ for $b\bar{b}$ events [3] using the median z position of tracks at their point-of-closest-approach to the IP in the $r\phi$ plane.

The measurements rely on a Monte Carlo simulation based on the JETSET 7.4 event generator [4] and the GEANT 3.21 detector simulation package [5] to determine the charge separation purity and to extract the lifetimes from the decay length distributions. The b -quark fragmentation follows the Peterson *et al.* parameterization [6]. B mesons (baryons) are generated with mean lifetime $\tau = 1.55$ ps ($\tau = 1.10$ ps). B meson decays are modelled according to the CLEO B decay model [7] tuned to reproduce the spectra and multiplicities of leptons, charmed hadrons, pions, kaons, and protons, measured at the $\Upsilon(4S)$ [8]. Semileptonic decays follow the ISGW model [9] including 23% D^{**} production. B baryon and charmed hadron decays are modelled using JETSET with, in the latter case, branching fractions tuned to existing measurements [10].

The initial step in the event selection is to select electron and muon candidates using the measured track parameters as well as measurements from the LAC and WIC respectively (see Ref. [11] for further details). To enhance the fraction of $Z^0 \rightarrow b\bar{b}$ events with little loss in efficiency, lepton candidates are required to have total momentum $p > 2$ GeV/c and momentum transverse to the nearest jet > 0.4 GeV/c (jets are found using the JADE algorithm [12] with $y_{cut} = 0.005$). These cuts yield a sample of $\sim 34,000$ event hemispheres, with an efficiency of $\sim 75\%$ for semileptonic B decays within $|\cos\theta| < 0.6$ determined from our Monte Carlo simulation.

The secondary vertex reconstruction proceeds separately for each event hemisphere containing a lepton, and uses a multi-pass algorithm that operates on those tracks that have at least one VXD hit and are not from identified γ conversions, or K_s^0 or Λ decays. Tracks are initially classified as primary unless their 3-D impact parameter significance with respect to the IP is $> 3.5\sigma$ and $p > 0.8$ GeV/c, in which case they are classified as secondary.

In the first pass, the hemisphere containing the lepton candidate is required to include no more than four secondary tracks (excluding the lepton) and a candidate D vertex is constructed using all such tracks (vertex cuts are defined below). The D trajectory, found from the D vertex and the total momentum vector of tracks included in the vertex, must intersect the lepton to form a valid one-prong B vertex solution. If this is successful, an attempt is made to form a two-prong B vertex by attaching one primary track to the

lepton near the point of intersection. This first pass identifies 91% of the final candidates. These candidates are allowed to be modified by searching for one or two primary tracks that can be added to the existing D vertex. This search is successful for 40% of the candidates. In case of multiple solutions, we select the one with the largest number of tracks and if more than one still remains, we select that with the smallest impact parameter between the D trajectory and the lepton or two-prong B vertex. A second pass is performed if no first pass candidate is identified. Here, a search is made for solutions in which one secondary track makes a valid two-prong B vertex with the lepton, the remaining secondary tracks form a D vertex, and the D trajectory intersects the B vertex. Multiple solutions are handled as described above.

The requirements to form a D vertex are: the number of tracks is ≤ 4 ; the absolute value of the charge ≤ 1 ; the mass (charged tracks assumed to be π 's) $< 1.98 \text{ GeV}/c^2$; the vertex displacement from the IP $> 4\sigma$ and $< 2.5 \text{ cm}$; and the vertex χ^2 (2,3,4 prongs) $< (4, 12, 20)$. The requirements to form a B vertex are: the absolute value of the total charge ($B+D$ tracks) ≤ 1 ; the mass $> 1.4 \text{ GeV}/c^2$; the observed decay length $> 0.08 \text{ cm}$ and $< 2.4 \text{ cm}$; and the momentum of the non-lepton track (if any) $> 0.4 \text{ GeV}/c$. The requirements for the D vertex to be linked to the B vertex are: the signed distance between D and B vertices $> 200 \mu\text{m}$; for one-prong B vertices, the distance of closest approach of the D trajectory to the lepton $< (130, 100, 70) \mu\text{m}$ for (2, 3, 4) prong D vertices; for two-prong B vertices, the three-dimensional impact parameter of the D trajectory with respect to the B vertex $< 200 \mu\text{m}$.

The algorithm yields 783 charged and 584 neutral semileptonic B decay candidates. The topological breakdown is given in Table 1. The efficiency for reconstructing a semileptonic B decay is estimated from the simulation to be 24% for decays with an identified lepton within $|\cos\theta| < 0.6$.

Monte Carlo studies indicate that the B^+ topology consisting of two-prong B and three-prong D vertices has poor B^+ purity due to the small $B^+ \rightarrow D^-\pi^+l^+\nu$ branching ratio and the large background from $B^0 \rightarrow D^{(*)-}l^+\nu$ decays. This is corroborated by the large fraction of decays with B vertex charge = 0 observed in the data for this topology. Therefore, this topology is rejected thereby reducing the charged sample to 634 candidates. These studies show that the remaining charged (neutral) sample is 97.4% (98.9%) pure in B hadrons with flavor contents of 66.6% B^+ , 22.9% B^0 , 5.5% B_s^0 , and 2.4% B baryons for the charged sample, and 19.5% B^+ , 60.2% B^0 , 14.8% B_s^0 , and 4.4% B baryons for the neutral sample. The sensitivity of

Table 1: Summary of reconstructed topologies, including the fraction of each topology in the combined charged and neutral sample for data and Monte Carlo simulation.

	<i>B</i> Vertex	<i>D</i> Vertex	Data	MC	
			# decays	Fraction	
$Q = \pm 1$	1 prong	2 prong	519	$(38.0 \pm 1.3)\%$	37.6%
	1 prong	4 prong	115	$(8.4 \pm 0.8)\%$	8.5%
	2 prong	3 prong	149	$(10.9 \pm 0.8)\%$	9.6%
$Q = 0$	1 prong	3 prong	341	$(24.9 \pm 1.2)\%$	26.8%
	2 prong	2 prong	175	$(12.8 \pm 0.9)\%$	13.6%
	2 prong	4 prong	68	$(5.0 \pm 0.6)\%$	3.9%

the analysis to the individual B^+ and B^0 lifetimes can be assessed from the 3:1 ratio of $B^+(B^0)$ over $B^0(B^+)$ decays in the charged (neutral) sample. The fraction of misidentified leptons is 7.0% (9.7%) for charged (neutral) candidates, as determined from the simulation. However, these are predominantly B decays with good charge purity.

As a check of the algorithm, the requirements on the charges of the B and D vertices are removed for Figs. 1(a) and 1(b). Figure 1(a) shows that, as expected, the charges of the lepton and D vertex are opposite for most reconstructed decays (provided the D vertex is charged). Furthermore, the charge distribution resulting from the lepton+slow transition pion vertex (from $D^{*(*)}$) shown in Fig. 1(b) indicates that the track combined with the lepton to form a two-prong B vertex most often has charge opposite that of the lepton, as expected for $B \rightarrow D^*l\nu$ and most $B \rightarrow D^{**}l\nu$ decays. Figure 1 also shows the total vertex momentum distribution obtained using the tracks from both B and D vertices, and the D vertex multiplicity distribution (with the nominal charge requirements on the vertices). Overall, there is agreement between the data and the Monte Carlo simulation.

The B^+ and B^0 lifetimes are extracted from the decay length distributions of the B vertices in the charged and neutral samples (see Fig. 2) using a binned maximum likelihood technique. These distributions are fitted simultaneously to determine the B^+ and B^0 lifetimes. For each set of parameter

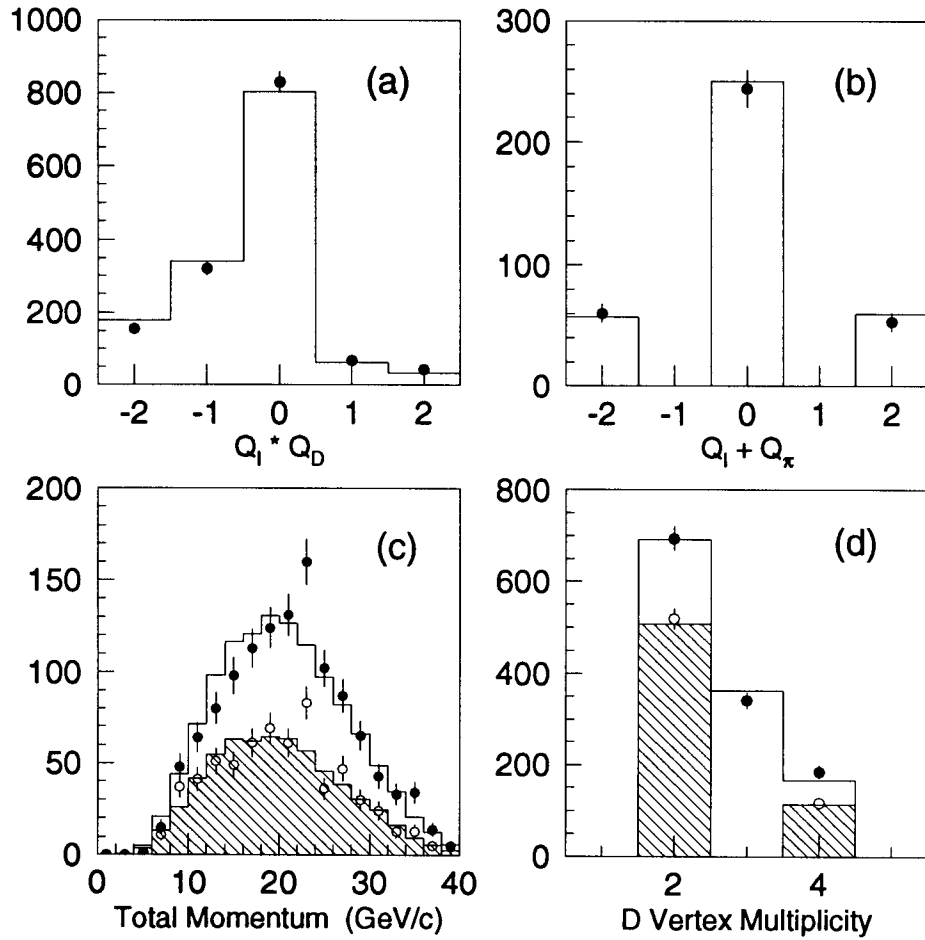


Figure 1: Distributions of (a) the product of lepton and D -vertex charges, (b) sum of lepton and slow transition pion charges for data (points) and Monte Carlo simulation (histograms) with no charge requirement at the B and D vertices. Distributions of (c) total momentum of the $B+D$ tracks and (d) D vertex multiplicity for data (solid circles are for total sample, open circles are for charged sample only) and Monte Carlo simulation (histograms are for total sample, shaded portions are for charged sample only).

values, Monte Carlo decay length distributions are obtained by reweighting entries from generated B^+ and B^0 decays in the original Monte Carlo decay length distributions with $W(t, \tau) = \left(\frac{1}{\tau} e^{-t/\tau}\right) / \left(\frac{1}{\tau_{gen}} e^{-t/\tau_{gen}}\right)$, where τ is the desired B^+ or B^0 lifetime, $\tau_{gen} = 1.55$ ps, and t is the proper time of each decay. The fit then compares the decay length distributions from the data with the reweighted Monte Carlo distributions. The fit yields

$$\begin{aligned}\tau_{B^+} &= 1.61^{+0.13}_{-0.12} \text{ ps}, \\ \tau_{B^0} &= 1.56^{+0.14}_{-0.13} \text{ ps}, \\ \tau_{B^+}/\tau_{B^0} &= 1.03^{+0.16}_{-0.14}.\end{aligned}$$

with a $\chi^2 = 78$ for 76 degrees of freedom.

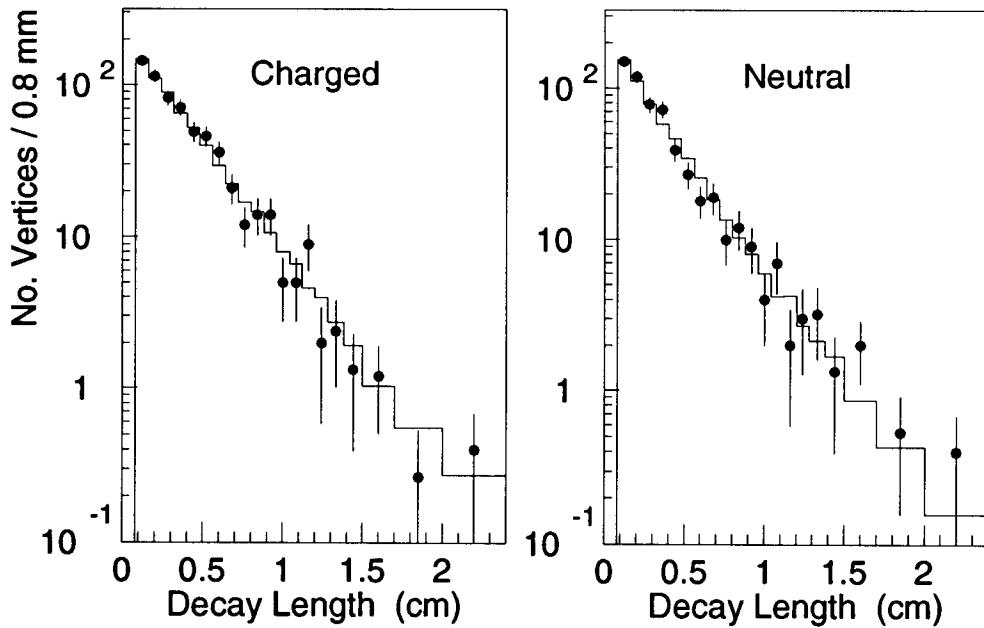


Figure 2: Decay length distributions for charged and neutral decays for data (points) and the Monte Carlo simulation corresponding to the best fit (histograms).

Systematic uncertainties due to detector and physics modeling, as well as those related to the fitting procedure, are described below and summarized in Table 2. A discrepancy between data and simulation in the fraction of tracks passing a set of quality cuts [3] is corrected for by removing 4% of the tracks from the simulation. In addition, a 0.9^{m-2} correction to the vertex reconstruction efficiency is applied, where m is the D vertex track multiplicity. The uncertainty due to the track finding efficiency is conservatively estimated as the full difference between fits with and without these corrections. The uncertainty due to tracking resolution is similarly taken to be

Table 2: Summary of systematic uncertainties in the B^+ and B^0 lifetimes and their ratio.

Systematic Error		$\Delta\tau_{B^+}$	$\Delta\tau_{B^0}$	$\Delta\frac{\tau_{B^+}}{\tau_{B^0}}$
		(ps)	(ps)	
Detector Modeling				
Tracking efficiency		0.017	0.029	0.023
Tracking resolution		0.020	0.030	0.033
Lepton misidentif.		0.006	0.007	<.003
Physics Modeling				
b fragmentation	0.700 ± 0.011	0.035	0.039	0.016
$\frac{BR(B \rightarrow D^{**}l\nu)}{BR(B \rightarrow Xl\nu)}$	0.230 ± 0.115	0.011	0.018	0.016
$BR(B \rightarrow D\bar{D}X)$	0.15 ± 0.05	0.009	0.008	0.011
B_s^0 fraction	0.115 ± 0.040	0.007	0.007	0.009
B baryon fraction	0.072 ± 0.040	0.008	0.016	0.006
B_s^0 lifetime	1.55 ± 0.10 ps	0.003	0.028	0.020
B baryon lifetime	1.10 ± 0.08 ps	<.003	0.007	0.005
D decay multipl.	Ref.[15]	0.014	0.009	<.003
D mom. mismatch		<.003	0.034	0.022
Monte Carlo and Fitting				
Fitting systematics		0.037	0.052	0.061
MC statistics		0.023	0.024	0.027
TOTAL		0.066	0.097	0.088

the difference between fits before and after smearing and shifting the track impact parameters in the rz plane to account for residual VXD misalignments [3]. The smearing by $\sigma = 20 \mu\text{m} / \sin\theta$ and shifts up to $20 \mu\text{m}$ are required to match the core of the impact parameter distribution observed in the data. No correction is required to the impact parameters in the $r\phi$ plane. The B^0 lifetime is more sensitive to the above uncertainties than the B^+ lifetime because they affect the relative abundance of the various topologies (listed in Table 1) and the amount of wrong-charge vertices at short decay length is higher for two-prong than for one-prong B vertex topologies. The rate of lepton misidentification is varied by $\pm 25\%$ in the simulation. It was checked that the lifetimes obtained in four different azimuthal regions are statistically consistent.

The b -quark fragmentation uncertainty includes contributions from shifting the mean value of the B hadron energy [13] and using a different fragmentation function shape [14]. As expected, this uncertainty affects the individual lifetimes but leaves the lifetime ratio relatively unaffected. Uncertainties in the B_s^0 and B baryon production and lifetimes contribute more significantly to the B^0 lifetime, and thus affect the lifetime ratio, due to the larger fraction of B_s^0 and B baryons in the neutral sample. Sensitivity to the branching ratio for decays involving $b \rightarrow c \rightarrow l$ transitions or for $B \rightarrow \tau\nu_\tau X$ decays is negligible. Similarly, uncertainties due to the charmed hadron lifetimes are negligible.

A slight discrepancy between data and simulation is observed in the vertex total momentum distribution for the neutral sample (see Fig. 1(c)). This mismatch is investigated by reweighting the Monte Carlo D vertex momentum distribution to match the data in both charged and neutral samples. Although the discrepancy may be attributed in part to the B decay modeling, we conservatively assign an uncertainty to be the difference between fits with and without reweighting.

The fitting uncertainties are estimated by varying the bin size and the minimum and maximum decay length cuts. Although the lifetimes obtained for each of these variations are statistically consistent, we conservatively assign an uncertainty equal to the root mean square value of all these results. This uncertainty dominates all others but is largely driven by the available statistics.

The final results are

$$\begin{aligned}\tau_{B^+} &= 1.61_{-0.12}^{+0.13}(\text{stat}) \pm 0.07(\text{syst}) \text{ ps}, \\ \tau_{B^0} &= 1.56_{-0.13}^{+0.14}(\text{stat}) \pm 0.10(\text{syst}) \text{ ps}, \\ \tau_{B^+}/\tau_{B^0} &= 1.03_{-0.14}^{+0.16}(\text{stat}) \pm 0.09(\text{syst}).\end{aligned}$$

These results complement those obtained with an inclusive topological technique [16], and are in agreement with previous measurements [2, 17] and with the expectation that the B^+ and B^0 lifetimes are nearly equal.

We thank the personnel of the SLAC accelerator department and the technical staffs of our collaborating institutions for their outstanding efforts.

References

- [1] I.I. Bigi *et al.*, in *B Decays*, edited by S. Stone (World Scientific, Singapore, 1994), p. 132.
- [2] D. Buskulic *et al.*, *Z. Phys.* **C71**, 31 (1996); P. Abreu *et al.*, *Z. Phys.* **C68**, 13 (1995), P. Abreu *et al.*, Report No. CERN-PPE/96-139, 1996; R. Akers *et al.*, *Z. Phys.* **C67**, 379 (1995); F. Abe *et al.*, *Phys. Rev. Lett.* **76**, 4462 (1996).
- [3] K. Abe *et al.*, *Phys. Rev.* **D53**, 1023 (1996).
- [4] T. Sjöstrand, *Comp. Phys. Comm.* **82**, 74 (1994).
- [5] R. Brun *et al.*, Report No. CERN-DD/EE/84-1, 1989.
- [6] C. Peterson *et al.*, *Phys. Rev.* **D27**, 105 (1983).
- [7] CLEO B decay model provided by P. Kim and the CLEO Collaboration.
- [8] B. Barish *et al.*, *Phys. Rev. Lett.* **76**, 1570 (1996); H. Albrecht *et al.*, *Z. Phys.* **C58**, 191 (1993); H. Albrecht *et al.*, *Z. Phys.* **C62**, 371 (1994); F. Muheim, in *Proceedings of the 8th Meeting Division of Particles and Fields, Albuquerque, August, 1994* (World Scientific, Singapore, 1995), Vol. 1, p. 851; M. Thulasidas, Ph.D thesis, Syracuse University, 1993;

- G. Crawford *et al.*, Phys. Rev. **D45**, 752 (1992); D. Bortoletto *et al.*, Phys. Rev. **D45**, 21 (1992).
- [9] N. Isgur, D. Scora, B. Grinstein, and M.B. Wise, Phys. Rev. **D39**, 799 (1989).
- [10] Particle Data Group, Phys. Rev. **D50**, Part I (1994).
- [11] K. Abe *et al.*, Phys. Rev. Lett. **74**, 2895 (1995).
- [12] S. Bethke *et al.*, Phys. Lett. **213B**, 235 (1988).
- [13] see for example, R. Akers *et al.*, Z. Phys. **C60**, 199 (1993); D. Buskulic *et al.*, Z. Phys. **C62**, 179 (1994); P. Abreu *et al.*, Z. Phys. **C66**, 323 (1995).
- [14] M. G. Bowler, Z. Phys. **C11**, 169 (1981).
- [15] D.Coffman *et al.*, Phys. Lett. **B263**, 135 (1991).
- [16] K. Abe *et al.*, Report No. SLAC-PUB-7266, 1996, submitted to Phys. Rev. Lett.
- [17] W. Adam *et al.*, Z. Phys. **C68**, 363 (1995); F. Abe *et al.*, Phys. Rev. Lett. **72**, 3456 (1994).